MCB
Journals.ASM.org

RBFOX2 Promotes Protein 4.1R Exon 16 Selection via U1 snRNP Recruitment

Shu-Ching Huang,[a,b] Alexander C. Ou,[a] Jennie Park,[a] Faye Yu,[a] Brian Yu,[a] Angela Lee,[a] Guang Yang,[a,b] Anyu Zhou,[a,b] and Edward J. Benz, Jr.[a,b,c]

Department of Medical Oncology, Dana-Farber Cancer Institute,[a] Department of Medicine, Brigham and Women's Hospital,[b] and Dana-Farber/Harvard Cancer Center, Harvard Medical School,[c] Boston, Massachusetts, USA

The erythroid differentiation-specific splicing switch of protein 4.1R exon 16, which encodes a spectrin/actin-binding peptide critical for erythrocyte membrane stability, is modulated by the differentiation-induced splicing factor RBFOX2. We have now characterized the mechanism by which RBFOX2 regulates exon 16 splicing through the downstream intronic element UGCAUG. Exon 16 possesses a weak 5′ splice site (GAG/GTTTGT), which when strengthened to a consensus sequence (GAG/GTAAGT) leads to near-total exon 16 inclusion. Impaired RBFOX2 binding reduces exon 16 inclusion in the context of the native weak 5′ splice site, but not the engineered strong 5′ splice site, implying that RBFOX2 achieves its effect by promoting utilization of the weak 5′ splice site. We further demonstrate that RBFOX2 increases U1 snRNP recruitment to the weak 5′ splice site through direct interaction between its C-terminal domain (CTD) and the zinc finger region of U1C and that the CTD is required for the effect of RBFOX2 on exon 16 splicing. Our data suggest a novel mechanism for exon 16 5′ splice site activation in which the binding of RBFOX2 to downstream intronic splicing enhancers stabilizes the pre-mRNA–U1 snRNP complex through interactions with U1C.

Alternative splicing is a eukaryotic regulatory mechanism that allows for the generation of numerous protein isoforms with often diverse biological functions from a single gene (4, 26, 41). It begins with the spliceosome, which is assembled stepwise by the addition of discrete small nuclear ribonucleoprotein particles (snRNPs) and numerous accessory non-snRNP splicing factors (23, 33). The excision of introns followed by the joining of exons depends on the recognition and usage of 5′ and 3′ splice sites (5′ ss and 3′ ss, respectively) by the splicing machinery (19, 34). The initial splicing step is comprised of 5′ ss recognition by U1 snRNP and binding of U2 auxiliary factor (U2AF) to the 3′ ss. These factors and additional proteins form the E or commitment complex, which bridges the intron and brings the splice sites close together. U2AF then recruits U2 snRNP to form the A complex. Subsequent binding of the U4-U6-U5 tri-snRNP and many other factors result in a fully assembled spliceosome that supports a series of rearrangements via RNA-RNA and RNA-protein interactions and activates the catalytic steps of cleavage, exon joining, and intron release (4, 26).

The splice site signals that define the 5′ ss and 3′ ss of an alternatively spliced exon are often weak. How and when they are used is believed to be modulated by a complex interplay of positive (splicing enhancers) and negative (splicing silencers) *cis* elements and *trans*-acting factors (4, 26). These form the basis for alternative splicing. Target prediction for specific splicing factors is difficult, largely due to the small size and degeneracy of splicing factor-binding motifs. An exception to this degeneracy is the hexanucleotide UGCAUG, which has been shown to be an important element for the splicing of several exons (3, 5, 14, 16, 20, 24, 25, 30, 31, 37, 45–47).

The RBFOX1 and RBFOX2 family of RNA-binding proteins specifically recognizes the UGCAUG element, and its members function as critical alternative splicing network regulators. There are thousands of potential RBFOX targets, with binding sites highly conserved across numerous vertebrate species (49). RBFOX proteins can either enhance or repress splicing, depending on their binding site locations, e.g., those within or adjacent to the target exons, and also contribute to the production of more complex splicing patterns. UGCAUG represses splicing when located upstream of the exon (22, 51) but activates splicing when located downstream (25, 31, 37, 43, 45–47). Exon 9* of the CaV1.2 L-type calcium channel contains both upstream and downstream RBFOX sites, as well as an RBFOX site within the exon itself. RBFOX-dependent repression of exon 9* requires RBFOX-binding elements within the exon and upstream intron (43). Mauger et al. (27) demonstrated that RBFOX2 interacted with members of the hnRNP H/F family to better compete with SF2/ASF for binding to exon IIIc of the fibroblast growth factor receptor 2 (*FGFR2*), thus favoring exon exclusion. Zhou and colleagues (51) showed that RBFOX1 and RBFOX2 proteins interacted with the upstream UGCAUG elements in a manner that blocked $U2AF^{65}$ binding to the 3′ ss upstream of exon 4 in calcitonin/CGRP pre-mRNA. However, the mechanism through which UG CAUG acts as an enhancer remains to be determined.

The 80-kDa erythrocyte protein 4.1R (4.1R) is the prototype of a diverse array of 4.1R isoforms. The expression of exon 16, which encodes peptides within the spectrin-actin-binding domain (SAB), which is critical for the mechanical stability of the red blood cell membrane (12, 18, 42), is tightly regulated during erythroid differentiation. Its deficiency enhances red cell membrane fragmentation and results in a hemolytic disorder termed "hered-

Received 12 October 2011 **Accepted** 2 November 2011
Published ahead of print 14 November 2011
Address correspondence to Shu-Ching Huang, shu-ching_huang@dfci.harvard.edu.
A. C. Ou, J. Park, and F. Yu contributed equally to this work.

doi:10.1128/MCB.06423-11

itary elliptocytosis" (44). Exon 16 is mostly absent in 4.1R mRNA of pre-erythroid cells but predominates in late erythroid cells (2, 7). Both RBFOX1 and RBFOX2 have been shown to bind to UG CAUG elements in the intron downstream of exon 16 and activate exon 16 splicing in HeLa cell (37). We have shown previously (46) that erythroid differentiation-induced RBFOX2 is an important regulator for the differentiation-specific exon 16 splicing switch.

In this study, we examined the molecular mechanism by which downstream intronic RBFOX2 binding enhances protein 4.1R exon 16 splicing. Exon 16 possesses a relatively strong 3′ ss but a weak 5′ ss. In addition, we found that impaired RBFOX2 binding reduced exon 16 inclusion in the presence of a weak 5′ ss, but not a strong 5′ ss. Mechanistically, RBFOX2 stabilizes or increases U1 snRNP recruitment to the weak 5′ ss through a direct interaction between its CTD and the zinc finger domain of U1C. These results suggest that binding of RBFOX2 to UGCAUG through its RRM domain may aid the recruitment of U1 snRNP to the weak 5′ ss through its interaction with U1 snRNP-associated U1C, providing a potential molecular mechanism for the enhancing function of this splicing factor.

MATERIALS AND METHODS

Plasmid constructs. All DNA constructs were made using standard cloning procedures and confirmed by sequencing.

The exon 16 wild-type (WT) minigene and mutant constructs comprised a three-exon (exons 13, 16, and 17) splicing cassette with a consensus 5′ ss (AA) or mutations in RBFOX2 binding sites (PNB) have been previously described (9). The double mutation AA/PNB construct was created using the QuikChange II XL site-directed mutagenesis kit (Stratagene), replacing the TT at positions +3 and +4 of the exon 16 5′ ss in the PNB minigene with AA.

For the E complex assembly construct, the 5′ ss of exon 13 (AAG/GT ATGT) was deleted from the WT and AA exon 16 minigene by using a two-step PCR strategy. The resultant products were then cloned into a pRC-CMV vector digested with NotI and XbaI to form WT_E and AA_E.

Ex16-weak 3′ ss constructs were created by changing the first nucleotide of exon 16 from A to G and replacing 7 nucleotides from positions −9 through −3 with the sequences CTAAACC and CTAAACA using the exon 16 AA minigene as a template and the QuikChange II XL site-directed mutagenesis kit to create AA1 and AA2, respectively. Similarly, positions −14 through −3 were replaced with the sequence CTGATCTA AACA to generate AA3.

The Ex16-MS2 construct was created by replacing RBFOX2-binding sequences in the exon 16 WT minigene with oligonucleotide 3MS2-S (5′-CGATCGTACACCATCAGGGTACGAGCTAGCCCATGGCGTACA CCATCAGGGTACGACTAGTAGATCTCGTACACCATCAGGGTACGC CGC-3′) comprising three copies of the binding site for the MS2 coat protein.

Psoralen cross-linking constructs consisting of sequences spanning 43 nucleotides (nt) of the 3′ end of exon 16 and 154 nt of its downstream intron were amplified from their respective minigenes and subsequently cloned with the NheI and XhoI sites in pcDNA3.1(+) (Invitrogen).

Fox/DUP and DUP with or without three copies of the intronic sequences spanning the first and second UGCAUG repeats (TGCATGCAA TTGCATG) downstream of 4.1R exon 16, respectively, were as described previously (46). AA/DUP was constructed by replacing the TG at positions +3 and +4 of the E2 5′ ss in the DUP minigene with AA.

RBFOX2 (GenBank accession number NM_001082579.1) was amplified from human $CD34^+$ RNA (StemCell Technologies, Inc.) with the primer set hFox2-S (5′-ATGGCGGAGGGCGCCCAGCCGCAGCA-3′) and hFox2-As (5′-TCAGTAGGGGGCAAATCGGCTGTAG-3′). The product was subsequently cloned in frame into the expressing vector pMSCV-FLAG, a pMSCV/puro (Clontech) derivative with 3 copies of the FLAG tag inserted upstream of the multiple cloning site. Full-length RBFOX2 (amino acids [aa]1 to 450) and its domain deletion constructs ΔNTD (aa 164 to 450), ΔRRM (aa 1 to 181 and 255 to 450), ΔCTD (aa 1 to 319), and CTD (aa 268 to 450) were cloned into pMSCV-FLAG to generate Fox2-FL/pMSCV, Fox2-ΔNTD/pMSCV, Fox2-ΔRRM/pMSCV, Fox2-ΔCTD/pMSCV, and Fox2-CTD/pMSCV, respectively. Similarly, Fox2/MS2 fusion protein constructs were made by cloning the full-length RBFOX2 or its domain deletion in frame between the FLAG tag and the nuclear localization signal of vector pCIMS2-NLS-FLAG (10) to generate Fox2-FL/pCIMS2, Fox2-ΔNTD/pCIMS2, Fox2-ΔRRM/pCIMS2, Fox2-ΔCTD/pCIMS2, and Fox2-CTD/pCIMS2. Full-length RBFOX2 (aa 1 to 450) and its individual domains NTD (aa 1 to 164), RRM (aa 164 to 268), and CTD (aa 268 to 450) were cloned into pEGFP to generate Fox2-FL/pEGFP, Fox2-NTD/pEGFP, Fox2-RRM/pEGFP, and Fox2-CTD/pEGFP, respectively, for intracellular localization studies. To produce recombinant RBFOX2 proteins, full-length RBFOX2 was cloned into pGEX-6p1 (GE Healthcare Life Sciences) and pcDNA3.1-T7 tag vector (Novagen) to generate Fox2-FL/GST and Fox2-FL/T7, respectively. Sequences encoding the first 50 amino acids of RBFOX2 were cloned in pGEX-6p1 to generate Fox2-N50/GST and were used as an antigen for the production of RBFOX2-specific antibodies.

U1C (GenBank accession number NM_011432) was amplified from murine erythroleukemia cell (MELC) mRNA with the primer set mU1C-S (5′-ATGCCCAAGTTTTATTGTGACTACTGTGA-3′) and mU1C-As (5′-TTATCTGTCTGGCCGGGTCATGCCA-3′) and cloned into pGEX-6p1 to generate U1C/GST. The zinc finger domain of U1C (aa 1 to 38) was cloned into pGEX-6p1 to generate U1C-ZnFinger/GST. Full-length U1C (aa 1 to 159) and its domain deletion constructs ΔZnFinger (aa 39 to 159) and ZnFinger (aa 1 to 38) were cloned into pMSCV-FLAG to generate U1C-FL/pMSCV, U1C-ΔZnFinger/pMSCV, and U1C-ZnFinger/pMSCV, respectively.

Cell culture and transfection. MELC, HeLa, and HEK293 cells were cultured in Dulbecco's modified Eagle's medium supplemented with 0.1 mM nonessential amino acids, 1.0 mM sodium pyruvate, and 10% fetal bovine serum (Sigma). Cells were transfected with Lipofectamine 2000 (Invitrogen) according to the manufacturer's instructions. Exon 16 minigene and RBFOX2 expression stable lines were selected with 800 μg/ml G418 and 2.0 μg/ml puromycin, respectively.

RT-PCR analyses. Reverse transcription-PCR (RT-PCR) analysis of splicing products was performed using a limiting cycle amplification protocol that yields the PCR product within its linear range (9). RNAs from exon 16- or DUP-minigene-transfected cells were reverse transcribed using the SP6 primer. PCRs were performed with Ex13-S (5′-AGAGCCCA CAGAAGCATGGA-3′) and Ex17-As (5′-GTGTGTAGATAAGCCCTTG TCCCA-3′) for exon 16-based minigenes and with DUP-ex1-S (5′-AAG GTGAACGTGGATGAAGTTGGT-3′) and DUP-ex3-As (5′-ACAGATC CCCAAAGGACTCAAAGAAC-3′) for DUP-based minigenes. Spliced products were fractionated on 2% agarose gels or 7.5% DNA polyacrylamide gels and quantified using analytic software from the ChemiImager 5500 system (Alpha Innotech Co.). For each construct, two transfections were performed for each experiment. Each experiment was repeated three times, and standard deviations were determined.

GST pulldown assays. Glutathione *S*-transferase (GST), Fox2/GST, and U1C/GST fusion proteins were affinity purified via coupling to glutathione-Sepharose beads (GE Healthcare) according to the manufacturer's protocol. HEK293 cells were transfected with the pMSCV-FLAG vector, full-length RBFOX2, or RBFOX2 domain deletion constructs in pMSCV-FLAG. FLAG-tagged proteins were purified from transfected cells using the FLAG M purification kit (Sigma). Five micromolar GST or U1C/GST fusion proteins were incubated with 5 μM Fox2-FLAG in 60 μl of binding buffer (20 mM Tris-HCl, 200 mM NaCl, 1 mM EDTA, 0.5% NP-40; pH 8.0) at 4°C for 2 h. The protein mix was incubated with 60 μl of glutathione-agarose beads for an additional 1 h. The beads were then washed 4 times with a wash buffer (20 mM Tris-HCl, 20 mM KCl, 0.1% Triton X-100, 1 mM dithiothreitol; pH 8.0). The presence of Fox2-FLAG

bound to U1C was detected by Western blotting with an anti-FLAG antibody (Ab).

Spliceosome assembly reactions and analysis. Nuclear extract was incubated at room temperature for 20 min to deplete ATP and then used for prespliceosomal complex assembly. For assembly of the E complex, 5 ng of ^{32}P-labeled pre-mRNA transcript was incubated at either 0 or 30°C in 25-μl splicing reaction mixtures lacking $MgCl_2$ in ATP-depleted nuclear extracts (29). Where indicated, purified RBFOX2 protein was added to the reaction mixtures prior to incubation. The assembled RNA-protein complexes were fractionated in 1.5% low-melting-point agarose gels, fixed in 10% acetic acid and 10% methanol for 30 min, dried, and exposed to X-ray film (8).

Psoralen cross-linking and primer extension assays. Pre-mRNA substrates for psoralen-mediated UV cross-linking were produced from linearized plasmids by transcription with T7 RNA polymerase (Amersham Pharmacia Biotech) in the presence of a Ribo m^{7}G cap analog (Promega) and [α-^{32}P]NTP (PerkinElmer). HeLa and MELC nuclear extracts were prepared as described previously (11).

Psoralen cross-linking reactions were carried out as described previously (52) using the wt, aa, pnb, aa/pnb psoralen cross-linking transcripts. RNase H-mediated inactivation of U1 snRNP was performed as described previously (28) by incubating the nuclear extract with RNase H and an oligodeoxynucleotide complementary to positions 1 to 15 of U1 snRNA before cross-linking. Alternatively, the cross-linked RNA was purified and subsequently incubated with oligodeoxynucleotide complementary to positions 66 to 75 of U1 snRNA and digested with RNase H (21). The complementation assays for psoralen cross-linking were performed using MELC nuclear extracts with the addition of purified recombinant RBFOX2. The cross-linked products were analyzed on 5% polyacrylamide gels containing 8.3 M urea and quantified by phosphorimager analysis (Molecular Dynamics). Three independent experiments were performed for each transcript, and standard deviations were determined.

The cross-linked site was mapped by primer extension using an oligonucleotide (5′-GAATGCAGAAGGTTCCAG-3′) complementary to nucleotides 37 to 54 of the intron downstream of exon 16. Primer extension was carried out on RNA gel purified from cross-linked reactions in which the wt and aa RNA were incubated in either mock-treated or oligo-(U1 1-15)-treated extracts. Dideoxy sequencing reactions using the same oligonucleotide for primer extension and plasmid templates for psoralen cross-linking were performed using the sequencing kit from the Sequenase version 2.0 DNA sequencing kit from GE Healthcare.

Coimmunoprecipitation and immunoblotting. Coimmunoprecipitation of RBFOX2 and U1 snRNP proteins was performed as described previously (13) using nuclear extracts purified from either Fox2/pMSCV- or U1C/pMSCV-transfected MELC or HEK293 cells, producing exogenously expressed Fox2-FLAG or U1C-FLAG proteins, respectively. Nuclear extracts were incubated with anti-FLAG, anti-Fox2, anti-U1C, anti-U1 70K, or control IgG bound to protein A-Sepharose beads. The immunoprecipitated samples were examined for the presence of Fox2-FLAG, U1C-FLAG, and U1 70K with the respective antibodies.

Anti-Fox2 and anti-U1C polyclonal antibodies were raised against Fox2-N50/GST (the first 50 amino acids of RBFOX2) and U1C-GST fusion proteins, respectively. There is no cross-reactivity between anti-Fox2 and anti-U1C antibodies, as the anti-Fox2 antibody detected a protein of molecular mass ~60 kDa while anti-U1C detected a protein of molecular mass ~20 kDa. The presence of exogenously expressed Fox2-FLAG and U1C-FLAG proteins was detected with an anti-FLAG Ab (Sigma) using the enhanced chemiluminescence detection kit (Amersham Pharmacia). Anti-U1 70K Ab was purchased from Santa Cruz Biotechnology, Inc. Anti-β-actin antibody (Sigma) served as a loading control.

Indirect immunofluorescence and imaging. HeLa cells were transfected with the pEGFP vector, Fox2-EGFP, or individual RBFOX2 domains in the pEGFP vector and subjected to immunofluorescence staining with anti-SC35 antibody as described previously (39). The endogenous RBFOX2 were stained using an anti-Fox2 specific antibody. All samples were counterstained with 4′,6-diamidino-2-phenylindole (DAPI). The samples were viewed with a Zeiss Axiovert 200 M inverted microscope. The images were collected using SlideBook4 software and processed using Photoshop software (Adobe Systems, Inc.).

RESULTS

RBFOX2 facilitates exon 16 weak 5′ ss selection. We showed previously (46) that the erythroid differentiation-specific 4.1R exon 16 splicing switch is mediated by a differentiation-inducible RBFOX2 isoform. To understand how RBFOX2 exerts its positive effect on exon 16 splicing, we first analyzed the strength of exon 16 5′ ss and 3′ ss by using the Analyzer splice tool (http://ibis.tau.ac.il/ssat/SpliceSiteFrame.htm), which uses an algorithm to calculate the scores of donor and acceptor sequences (40). Exon 16 possesses a weak 5′ ss; it diverges from the consensus at positions +3 and +4, where TT are present instead of A[G]A, although it has the highly invariable GT at positions +1 and +2. The wild-type 5′ ss (GAG/GTTTGT) has a score of 76.85, while the 3′ ss (TTTCATTTTCACAG/A) is relatively stronger at 90.17; the reference consensus 5′ ss (CAG/GTAAGT) and 3′ ss (TTTTTTTTTTTCAG/G) sequences have a score of 100. A second splice site score calculation program (http://rulai.cshl.edu/new_alt_exon_db2/HTML/score.html) from Cold Spring Harbor Laboratory has a maximum 3′ score of 14.2 for the consensus 3′ ss (TTTTCCCTCCAG/G) and a maximum 5′ score of 12.6 for the 5′ ss (AAG/GTAAGT). The mean scores of the 3′ ss and 5′ ss for constitutive exons are 7.9 and 8.1, respectively. Exon 16 3′ ss had a score of 8.2, while the 5′ ss score was 4.6. Both programs suggest that exon 16 has a weak 5′ ss but a strong 3′ ss.

To identify whether RBFOX2 enhances exon 16 splicing by improving the recognition of the weak 5′ ss by U1 snRNP, we examined the relationships between RBFOX2 binding and the strength of the 5′ ss on exon 16 inclusion. We constructed mutated exon 16 minigenes that either strengthened the 5′ ss (AA), abolished the RBFOX2 binding sites (PNB), or contained both of the aforementioned modifications (AA/PNB) (Fig. 1A). We then examined exon 16 expression in transfected cells in the absence or presence of exogenous RBFOX2 expression. We tested constructs in both HeLa and MELC, because we found that RBFOX2 expression is cell type specific. Using an anti-Fox2 specific antibody, a band at ~64 kDa was detected in both MELC and HeLa cells. However, an additional thicker band at ~60 kDa was detected in HeLa cells but not in MELC (Fig. 1B).

In MEL, the WT minigene replicated the endogenous splicing pattern with ~18% exon 16 inclusion. Inclusion increased to ~54% in response to exogenous RBFOX2 expression (Fig. 1C, WT lanes). In contrast, the AA construct with the consensus 5′ ss resulted in ~95% exon 16 inclusion, regardless of whether RBFOX2 was overexpressed (Fig. 1C, AA lanes). Based on these findings, we explored the possibility that the strong 5′ ss can overcome the lack of RBFOX2-binding sites, thus obliterating the need for RBFOX2 to facilitate exon 16 splicing. The PNB construct with the WT 5′ ss and mutations in RBFOX2-binding sites reduced exon 16 inclusion to ~11% and abolished its ability to respond to exogenous RBFOX2 expression (Fig. 1C, PNB lanes). In contrast with the behavior of the PNB mutant, the presence of the consensus 5′ ss in AA/PNB overrode the effect of the RBFOX2 mutations and stimulated nearly complete exon 16 inclusion regardless of the expression levels of RBFOX2 (Fig. 1C, AA/PNB lanes).

In HeLa cells, the WT minigene has higher basal (~70%) exon

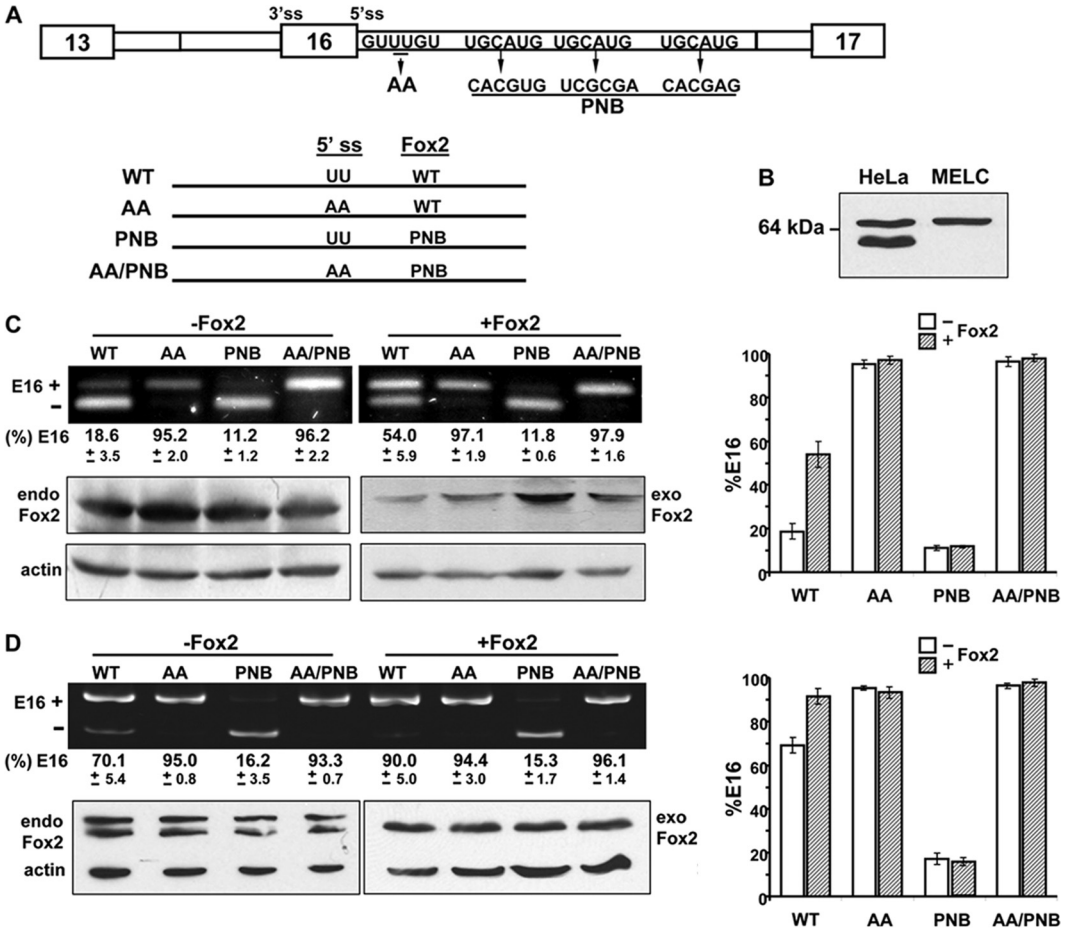

FIG 1 RBFOX2 facilitates exon 16 weak 5′ ss selection. (A) Schematic of exon 16 minigene and mutant derivatives used to test the relationships between RBFOX2-binding sites and the strength of the 5′ ss. Reporters consisting of either the wild-type (UU) or the consensus (AA) 5′ ss together with the wild-type (WT) or mutated RBFOX2 (PNB) binding sites are indicated. (B) Cell-line-specific expression of RBFOX2 in HeLa cells and MELC. HeLa cell lysates (50 μg) and MELC lysates (100 μg) were analyzed in a Western blot assay using an anti-Fox2-specific antibody. (C) RBFOX2 exerts a significant positive effect on exon 16 inclusion in the presence of a weak 5′ ss; impaired RBFOX2 binding reduces exon 16 inclusion in the context of the weak 5′ ss but not the strong 5′ ss. MELC were transfected with minigenes in the absence or presence of RBFOX2 and harvested 24 h after transfection. Semiquantitative RT-PCR was performed to determine the relative abundance of exon 16 by densitometric analysis. Mean values ± standard deviations (SD) of three independent experiments are shown. Anti-Fox2 and anti-FLAG Western blot results indicate the expression levels of endogenous and exogenous RBFOX2 proteins, respectively. β-Actin served as the loading control. The bar graph presents the densitometric analyses of the percentages of exon 16 inclusion from the three experiments performed (means ± SD). (D) Similar analyses as shown in panel C were performed on HeLa cells transfected with the same reporters in the absence or presence of RBFOX2.

16 inclusion, which coincides with a higher level of RBFOX2 expression. The inclusion increased to ~90% in response to RBFOX2 expression (Fig. 1D, WT lanes). Similar to that in MELC, the AA construct resulted in ~95% exon 16 inclusion regardless of the expression levels of RBFOX2 (Fig. 1D, AA lanes). The PNB construct reduced exon 16 inclusion to ~16% and did not respond to exogenous RBFOX2 expression (Fig. 1D, PNB lanes). The presence of the consensus 5′ ss in AA/PNB also superseded any effect of the RBFOX2 mutations, leading to nearly full exon 16 inclusion despite the expression levels of RBFOX2 (Fig. 1D, AA/PNB lanes).

Taken together, these results indicate that RBFOX2-binding sequences are important for mediating the effect of RBFOX2 on exon 16 splicing only in the presence of the weak 5′ ss. Consistent with a role for proteins in stabilizing U1 snRNP binding (21), RBFOX2 had little impact when the 5′ ss of exon 16 was strengthened by increasing complementarity with U1 snRNA.

UGCAUG activated splicing from a weak 5′ ss in a test DUP4-1 reporter system. To further investigate the direct effect of UGCAUG on the weak 5′ ss of alternatively spliced exons, we examined it in the context of a neutral reporter system, DUP4-1 (31). DUP4-1 produces an exon 1 and 3 product in the absence of added splicing enhancers (Fig. 2A). Similar to the 5′ ss of exon 16, the 5′ ss of the internal exon E2 is relatively weak, with a UG instead of the consensus AA at positions +3 and +4 and a score of 79.01 for the site. DUP4-1 thus provides a system for assaying the relationships between RBFOX2 and the various 5′ ss strengths in promoting E2 inclusion.

We constructed DUP minigenes containing either three copies of the intronic sequences spanning the first and second RBFOX2-binding sites of 4.1R exon 16 downstream of the target exon E2 (Fox/DUP) or consensus 5′ ss (AA/DUP) (Fig. 2A). We then examined E2 expression in transfected HeLa cells. DUP produced a product with complete E2 exclusion (Fig. 2B). Consistent with our

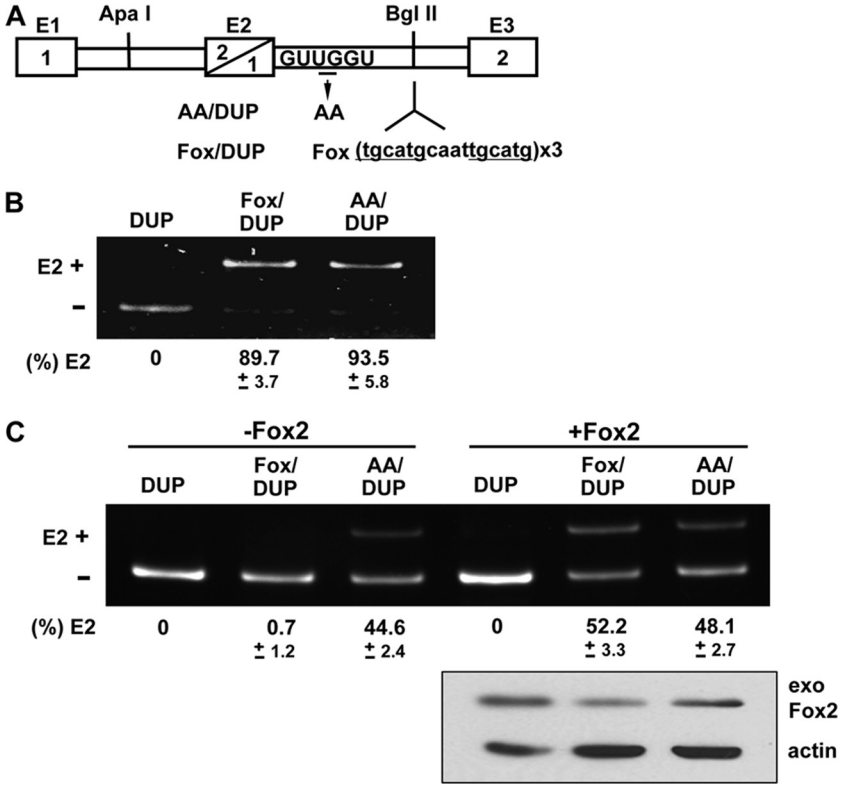

FIG 2 UGCAUG activates a DUP4-1 reporter gene 5′ splice site *in vivo*. (A) Schematic of the DUP4-1 minigene. DUP exon 1 is β-globin exon 1, and exon 3 is β-globin exon 2. The diagonal line in the second exon indicates a fusion between the first and second β-globin exons to make a 33-nucleotide hybrid exon (E2). A Fox/DUP construct was created in which three copies of RBFOX2-binding sequences (TGCATGCAATTGCATG) were inserted downstream of E2. AA/DUP has a consensus 5′ ss with AA in the positions +3 and +4 of 5′ ss. (B) Splicing patterns of DUP, Fox/DUP, and AA/DUP in HeLa cells. HeLa cells were stably transfected with the indicated constructs. RNAs were isolated and analyzed for E2 expression by RT-PCR. +E2, spliced products with E2; −E2, spliced products without E2; (%) E2, percentage of spliced products that include E2. (C) Splicing patterns of DUP, Fox/DUP, and AA/DUP in the absence or presence of RBFOX2 in MELC. Expression of exogenously expressed RBFOX2 was analyzed by Western blotting using an anti-FLAG antibody. β-Actin served as the loading control.

earlier report (46), the insertion of RBFOX2-binding sites promoted ~89.7% E2 inclusion (Fig. 2B). AA/DUP with a consensus 5′ ss resulted in ~93.5% E2 inclusion in the absence of RBFOX2-binding sites (Fig. 2B), suggesting that a strong 5′ ss overcomes the lack of RBFOX2-binding sites in promoting inclusion of E2.

We showed previously (46) that UGCAUG repeats activate DUP E2 splicing in an erythroid differentiation stage-specific manner in MELC. While there is no E2 inclusion in undifferentiated MELC, an ~20% inclusion was noted in differentiated MELC, which was most likely due to an upregulation of RBFOX2 expression in differentiated cells. Consistent with this early observation, E2 was excluded in the absence of exogenously expressed RBFOX2 (Fig. 2C, -Fox2, lane Fox/DUP). E2 showed an ~52% inclusion in the presence of RBFOX2 in Fox/DUP (Fig. 2C, +Fox2, lane Fox/DUP). Similar to the AA/DUP results in HeLa cells, strengthening the weak 5′ ss with AA overcame the requirement of RBFOX2 and enhanced E2 inclusion to ~45% regardless of the presence of exogenously expressed RBFOX2 (Fig. 2C, -Fox2 and +Fox2, lanes AA/DUP). Taken together, these results indicate that a strong 5′ ss does not require RBFOX2 binding in both the exon 16 and DUP4-1 system. However, cell-type-specific expression levels of RBFOX2 play a role in the degree of regulation.

RBFOX2-mediated splicing enhancement is weak 5′ ss dependent. The observations that RBFOX2 stimulates splicing in the presence of a weak 5′ ss but not a strong 5′ ss suggest that RBFOX2 regulates splicing in a 5′ ss-dependent manner. To investigate this possibility, we first ruled out the possibility that the effect of RBFOX2 depended on the 3′ ss as well as the 5′ ss.

We made exon 16 minigenes with weak 3′ ss by replacing several sequences at the 3′ ss that reduced 3′ ss scores from the original AA (90.17%) to AA1 (79.67%), AA2 (69.95%), and AA3 (64.76%) (Fig. 3A). The replacements significantly affected exon 16 inclusion, reducing it from 96.6% to 62%, 53.9%, and 48.1% for AA1, AA2, and AA3, respectively (Fig. 3B, -Fox2). The degree of exon 16 inclusion reduction correlated with gradually weakened 3′ ss.

We then examined whether the mutated minigenes would still be responsive to RBFOX2 by cotransfecting them with RBFOX2 into HeLa cells. Exogenous RBFOX2 proteins were expressed; however, no changes in the splicing pattern were detected (Fig. 3B, +Fox2). The addition of RBFOX2 did not improve exon 16 splicing under these conditions, suggesting that RBFOX2 is not needed once U1 is bound to the strong 5′ ss. Thus, the effect of RBFOX2 on exon 16 minigene pre-mRNA processing involves a weak 5′ ss-dependent mechanism, regardless of the strength of the 3′ ss.

RBFOX2 enhances formation of the prespliceosomal E complex. The observation that RBFOX2 exerted its effect through the 5′ ss (Fig. 1 to 3) prompted us to examine whether RBFOX2 participates in the first step of prespliceosomal complex assembly. For spliceosome assembly analysis, the 5′ ss of the upstream exon 13

A

Construct	Exon 16 3' splice site	3' ss score
AA	TTTCATTTTCACAG/A	90.17
AA1	TTTCACTAAACCAG/G	79.67
AA2	TTTCACTAAACAAG/G	69.95
AA3	CTGATCTAAACAAG/G	64.76

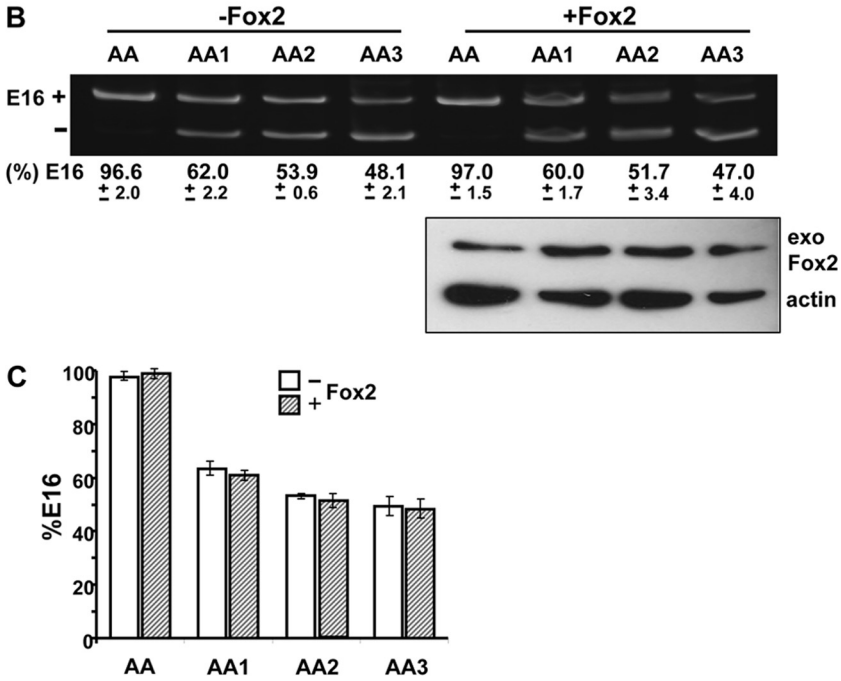

FIG 3 RBFOX2-mediated splicing enhancement is weak 5′ ss dependent. (A) 3′ ss weakened forms of exon 16 minigenes were constructed by replacing the sequences in the AA minigene with the underlined sequences, which resulted in 3′ ss score reductions. (B) RBFOX2 exerts no splicing effect on exon 16 inclusion when a strong 5′ ss is present. HeLa cells were transfected with the indicated minigenes in the absence or presence of RBFOX2. RNAs isolated were analyzed by RT-PCR for the relative abundance of exon 16 by densitometric analysis. Mean values ± standard deviations (SD) of three independent experiments are shown. Anti-FLAG Western blot assays indicated the expression levels of exogenous RBFOX2 proteins. β-Actin served as the loading control. (C) A bar graph presenting the densitometric analyses of the percentages of exon 16 inclusion from the three experiments performed (means ± SD).

was deleted from both AA and WT exon 16 minigenes (Fig. 4A) to ensure that splicing occurred only on the downstream intron and that the transcript assembled into a single spliceosome. The E complex formation is ATP independent and occurs at 30°C but not at 4°C (8). We incubated WT_E and AA_E transcripts in ATP-depleted MELC nuclear extracts in the absence or presence of purified RBFOX2 and analyzed subsequent E complex formation.

When incubated at 30°C for 40 min in the absence of supplemental RBFOX2, the AA_E transcript assembled an E complex, whereas the WT_E transcript did not form an E complex (Fig. 4B). However, the WT_E transcripts responded to the addition of RBFOX2 in a dose-dependent manner to yield E complex formation. The addition of RBFOX2 at 4 ng/μl to WT_E transcripts resulted in an assembled E complex with the same intensity as that of the AA_E transcript (Fig. 4B). Thus, RBFOX2 aided spliceosome assembly when a weak 5′ ss and RBFOX2-binding sites were present.

RBFOX2 aids in the recruitment of U1 snRNP to the weak exon 16 5′ splice site. The observation that RBFOX2 only exerts its effect and helps with E complex assembly on a weak 5′ ss suggests that RBFOX2 may assist in the recruitment of U1 snRNP to the weak 5′ ss. Early recognition of 5′ ss involves a base-pairing interaction with the 5′ end of U1 snRNA. We performed psoralen-mediated UV cross-linking assays to examine U1 snRNP recruitment to RNA. The substrates consisted of sequences spanning 43 nt of the 3′ end of exon 16 and 154 nt of the intron downstream of exon 16 with differing strengths of 5′ ss and RBFOX2-binding sites. As we did for the exon 16 minigene constructs used for analyzing the relationship between the 5′ ss strength and RBFOX2 binding (Fig. 1A), we made UV cross-linking constructs that were comprised of a combination of a weak or a consensus 5′ ss with the WT or mutated (PNB) RBFOX2 binding sites. They are referred to as wt, pnb, aa, and aa/pnb (Fig. 5A).

Psoralen-dependent cross-linked species were detected in both HeLa (Fig. 5B) and MELC nuclear extracts (data not shown). The products from wt and pnb substrates migrated more slowly than those of the aa and aa/pnb substrates. To determine the identity of the cross-linked species, we performed RNase H digestion using various anti-snRNA specific DNA oligonucleotides. Incubation of nuclear extracts in the presence of DNA oligonucleotides complementary to positions 1 to 15 of U1 snRNA followed RNase H digestion and cross-linking inhibited cross-linking in all sub-

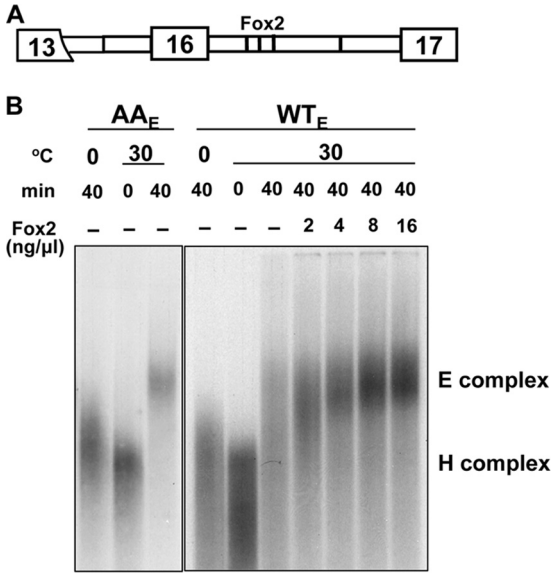

FIG 4 RBFOX2 enhances formation of the prespliceosomal E complex. (A) Schematic of the exon 16 minigene construct with the 5′ ss deleted from exon 13. (B) Spliceosomal complex formation on the AA_E and WT_E transcripts in the absence of ATP. AA_E and WT_E represent AA and WT minigenes in which the 5′ ss of exon 13 was deleted. AA_E and WT_E transcripts were incubated in ATP-depleted MELC nuclear extracts at 0 or 30°C for the indicated times. Purified recombinant RBFOX2 was added into WT_E, and subsequent E complex formation was analyzed on a 1.5% low-melting-point agarose gel, fixed, dried, and exposed to X-ray film.

strates (Fig. 5C, U1 1-15). Additionally, cross-linking followed by incubation with DNA oligonucleotides complementary to positions 66 to 75 of U1 snRNA and RNase H treatment produced cleaved U1 snRNA/exon 16 complexes (Fig. 5C, U1 66-75). None of the cross-linked species contained U2 snRNAs (data not shown). These results imply that the cross-linked species are U1 snRNP/exon 16 specific.

To map precisely the site of cross-linking, we performed primer extension analysis on gel-purified psoralen cross-linked products with an antisense primer located in an intron downstream of exon 16. We observed one prominent reverse transcriptase stop that corresponded to nucleotide C9 (the ninth nucleotide of the intron downstream of exon 16) in both wt and aa samples that were not treated with oligo-(U1 1-15) and RNase H (Fig. 5D, - lanes). In addition, a slowly migrating stop was also seen in the aa samples. When extracts were pretreated with oligo-(U1 1-15) prior to psoralen cross-linking (Fig. 5D, + lanes), the C9 stop was eliminated from both wt and aa samples, while the slowly migrating stop from the aa sample was not affected. The C9 stop thus appears to be a U1-specific cross-linking-dependent stop. The nt 1 to 11 of U1 snRNA are completely complementary to the nt −2 to +9 of the aa templates. This C9 primer extension stop was precisely what was predicted for the cross-linking of U1 snRNA to the 5′ ss of exon 16.

We constantly observed that wt cross-linked U1 was approximately 5-fold less efficient than that of aa (Fig. 5B). To achieve equal intensity of primer-extended bands, the amount of wt products used compared to the aa was 5-fold greater for the primer extension experiment in Fig. 5D. These results suggest that U1 RNA binds to the same site but with greater affinity for aa than for wt. The difference between the UU and AA dinucleotides at the 5′ ss most likely contribute to the electrophoretic migration differences of the products.

Mutations in the RBFOX2-binding site reduced the amount of cross-linked product, albeit at a low level, compared with that of the wt substrate (Fig. 5B). The presence of RBFOX2 mutated sequences in the aa/pnb substrate did not affect the ability of the strong 5′ ss to cross-link U1, as an intense cross-linked band was observed (Fig. 5B). These results support the notion that the effect of RBFOX2 is mediated through the weak 5′ ss, most likely through its ability to recruit U1 snRNP to the weak 5′ ss.

We further tested the direct effect of RBFOX2 on U1 snRNP recruitment to the WT or AA 5′ ss. Since HeLa nuclear extracts contain large amounts of RBFOX2, we performed these experiments using MELC nuclear extracts, which have much lower levels of RBFOX2 expression. The wt transcripts responded to the addition of RBFOX2 in a dose-dependent manner. Recruitment of U1 snRNP was enhanced approximately 5-fold when 16 ng/μl of purified recombinant RBFOX2 was added to reaction mixtures with wt substrates (Fig. 5E). In contrast, addition of RBFOX2 had no effect with pnb, aa, and aa/pnb substrates (Fig. 5E). These data suggest that the contribution of RBFOX2 in U1 snRNP recruitment is particularly critical when a weak 5′ ss is present. Therefore, RBFOX2 binding to the UGCAUG elements facilitates interaction with the U1 snRNP, allowing for weak 5′ ss recognition and subsequent splicing of exon 16.

RBFOX2 protein forms a complex with U1 snRNP-associated proteins. In addition to U1 snRNA, U1 snRNP is composed of seven different Sm proteins common to other snRNPs and three U1-specific proteins: U1 70K, U1A, and U1C (38). To further probe the interactions between RBFOX2 and U1 snRNP, RBFOX2 and U1-specific proteins were immunoprecipitated from MELC nuclear extracts expressing Fox2-FLAG or U1C-FLAG with anti-FLAG, anti-U1C, anti-Fox2, and anti-U1 70K antibodies and analyzed for the presence of the associated proteins. As shown in Fig. 6A, U1C-FLAG was detected in anti-Fox2 as well as anti-FLAG precipitates from U1C-FLAG extracts. In a reverse coimmunoprecipitation assay, Fox2-FLAG was also present in anti-FLAG and anti-U1C precipitates from Fox2-FLAG extracts (Fig. 6B). Similarly, U1 70K was detected in anti-FLAG precipitates, while Fox2-FLAG was detected in anti-U1 70K precipitates in Fox2-FLAG extracts (Fig. 6C). We were unable to detect any association between RBFOX2 and U1A in the coimmunoprecipitation assay. Nonetheless, these results demonstrate that RBFOX2 associates with U1 snRNPs.

The C-terminal domain of RBFOX2 directly interacts with the zinc finger domain of U1C. Fox proteins were identified as interactors of U1C in a yeast two-hybrid system (35). We thus examined whether RBFOX2 interacted with U1C directly in a GST pulldown assay. RBFOX2 consists of an NTD that harbors a putative nuclear localization signal (KRPR, amino acids 46 to 49), an RRM domain binding to UGCAUG sequences, and a CTD. U1C/GST or GST alone was incubated with the full-length Fox2-FL/FLAG or its domain-deletion FLAG fusions, i.e., without the NTD (Fox2-ΔNTD/FLAG), without the RRM (Fox2-ΔRRM/FLAG), without the CTD (Fox2-ΔCTD/FLAG), or with the CTD alone (Fox2-CTD/FLAG) (Fig. 7A) purified from transfected HEK293 cells and probed for the presence of FLAG fusion proteins. As shown in Fig. 7B, Fox2-FL/FLAG and its domain deletions Fox2-ΔNTD/FLAG, Fox2-ΔRRM/FLAG, and Fox2-CTD/FLAG, but

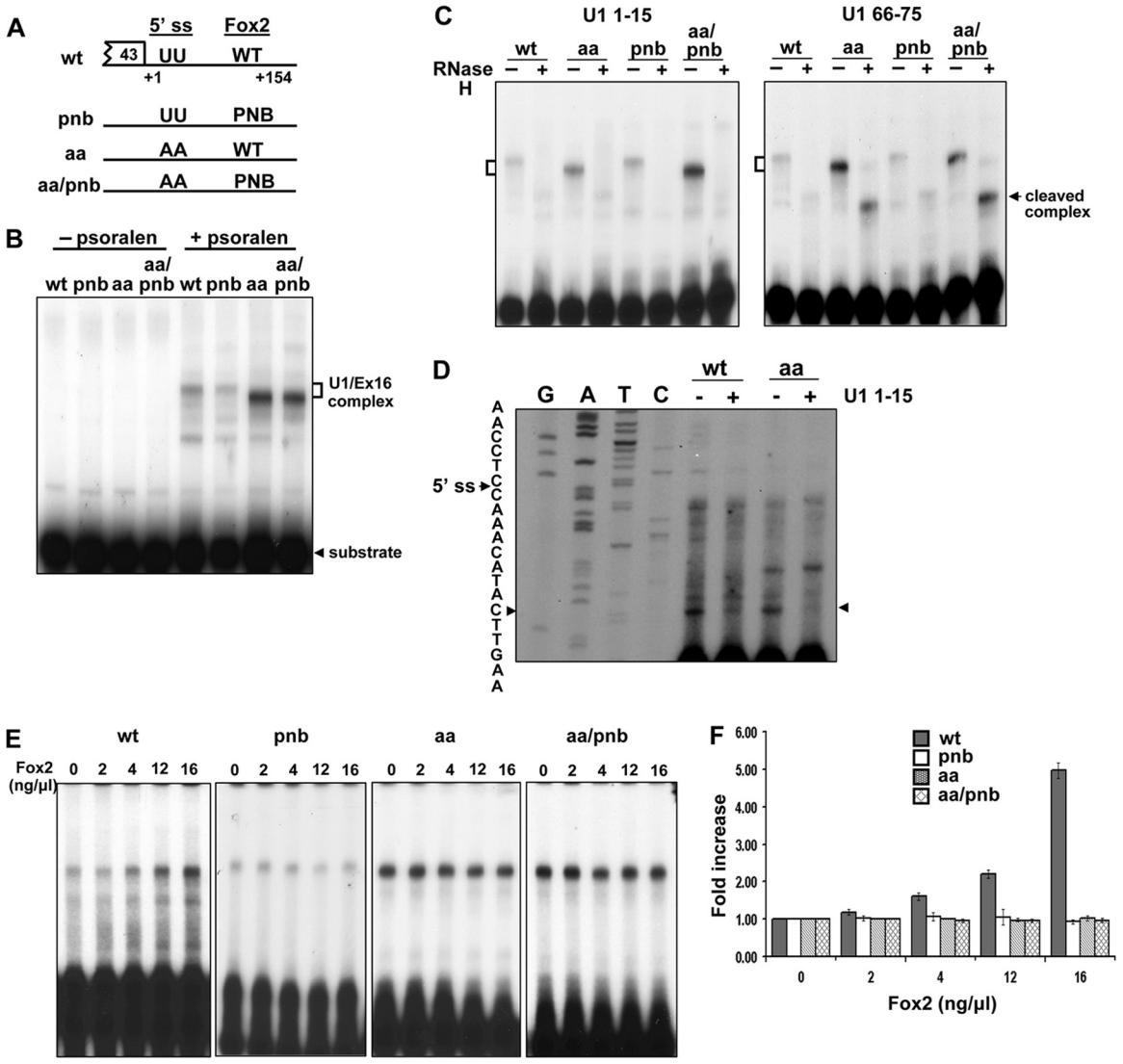

FIG 5 A psoralen cross-linking assay demonstrates activity of RBFOX2 in U1 snRNP recruitment. (A) Schematic representation of exon 16 wt substrate and mutant derivatives for psoralen-mediated cross-linking. The RNA substrates with either the wild-type (UU) or the consensus (AA) 5′ ss in conjunction with the WT or mutated RBFOX2 (PNB) binding sites are indicated. (B) Psoralen-dependent cross-linked species were detected upon incubation of ^{32}P-labeled RNA substrates in HeLa cell nuclear extracts. The positions of free substrates and U1 snRNA/exon 16 cross-linked complexes are indicated. (C) Validation of the U1 snRNA/exon 16 cross-linked bands performed by RNase H-mediated inactivation of U1 snRNP. (Left panel) Nuclear extracts were incubated with an oligonucleotide complementary to positions 1 to 15 of U1 snRNA and treated with RNase H before being cross-linked with substrates. (Right panel) RNAs were purified after cross-linking, incubated with oligonucleotides complementary to positions 66 to 75 of U1 snRNA, and digested with RNase H. Full-length cross-linked species are identified to the left of the gel; cleavage products are indicated to the right of the gel. (D) The psoralen cross-linked site mapped by primer extension using an antisense primer located 37 to 54 nucleotides downstream of exon 16. Primer extension was performed on gel-purified RNA from psoralen cross-linked reactions in which the wt and aa RNA were incubated in either mock-treated or oligo-(U1 1–15)-treated extracts. Arrow, U1-specific cross-linked stop; -, mock-treated; +, U1 1-15 treated. Dideoxy sequencing reactions were performed on the psoralen cross-linking plasmid templates using the same oligonucleotide primer. (E) A weak 5′ ss is central in establishing UGCAUG-dependent recruitment of U1 snRNP by RBFOX2. MELC nuclear extracts were used for psoralen cross-linking with substrates wt, pnb, aa, or aa/pnb in the presence of the indicated amounts of purified RBFOX2. (F) Bar graph presenting the densitometric analysis results of the folds of U1 snRNA/exon 16 cross-linked complexes over the respective control sample without the supplemental RBFOX2 from the three experiments performed (means ± standard deviations).

not Fox2-ΔCTD/FLAG, were detected with U1C/GST but not with GST using an anti-FLAG antibody. The interaction of RBFOX2 with U1C is most likely through the CTD of RBFOX2, since U1C/GST pulled down CTD-containing fusions but not the fusions lacking the CTD (Fig. 7B). Since splicing factors can also bind to RNA, we also examined whether the interaction was RNA mediated by performing the GST pulldown reactions in the presence or absence of RNase. Both the full-length and CTD of RBFOX2 interacted with U1C in an RNase-independent manner (Fig. 7C).

Subsequently, we looked to determine the region of U1C (Fig. 7A) responsible for the RBFOX2 interaction in pulldown assays. U1C and U1C-ΔZnFinger (U1C lacking the zinc finger domain) expressed as FLAG fusions were purified from transfected

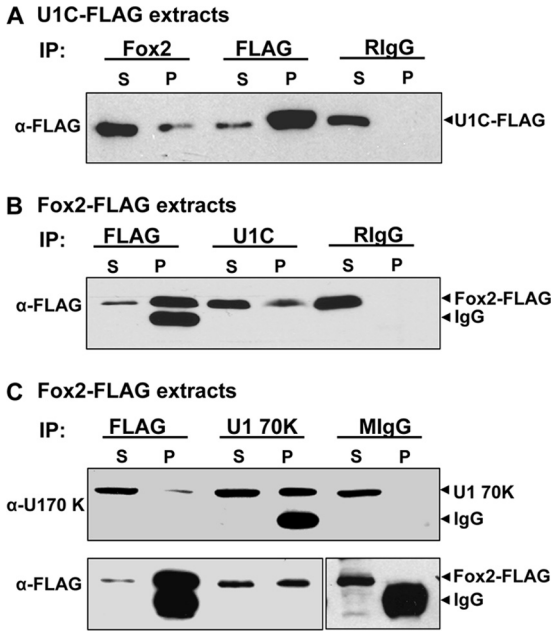

FIG 6 RBFOX2 associates with U1 snRNP. MELC nuclear extracts isolated from U1C-FL/pMSCV- or Fox2-FL/pMSCV-transfected cells, expressing U1C-FLAG or Fox2-FLAG, respectively, were subjected to immunoprecipitation using anti-FLAG, anti-Fox2, anti-U1C, and anti-U1 70 K antibodies and probed for the presence of associated proteins with anti-FLAG and anti-U1 70K antibodies. RIgG (rabbit IgG) and MIgG (mouse IgG) served as immunoprecipitation controls. (A) Anti-Fox2, anti-FLAG, and RIgG immunoprecipitates from U1C-FLAG extracts were immunoblotted with an anti-FLAG Ab for the presence of coprecipitated U1C-FLAG. (B) Anti-FLAG, anti-U1C, and RIgG immunoprecipitates from Fox2-FLAG extracts were immunoblotted with an anti-FLAG Ab for the presence of coprecipitated Fox2-FLAG. (C) Anti-FLAG, anti-U1 70K, and MIgG immunoprecipitates from Fox2-FLAG extracts were immunoblotted with an anti-U1 70K Ab (upper panel) and anti-FLAG Ab (lower panel) for the presence of coprecipitated U1 70 K and Fox2-FLAG, respectively. S, immunoprecipitation (IP) supernatant; P, IP beads.

HEK293 cells, incubated with Fox2/GST or GST, and probed for the presence of FLAG fusions. As shown in Fig. 7D, the full-length U1C/FLAG but not the U1C-ΔZnFinger interacted with Fox2/GST (Fig. 7D, U1C and ΔZnFinger). Due to the difficulty in purifying ZnFinger/FLAG, we expressed the zinc finger domain as a GST fusion and tested this in pulldown assays using Fox2-CTD/FLAG fusions. It is most likely that U1C interacts with Fox2-CTD through the zinc finger domain of U1C, as the ZnFinger/GST pulled down Fox2-CTD (Fig. 7D). These results suggest that binding of RBFOX2 to UGCAUG through its RRM domain may help recruitment of U1 snRNP to the weak 5′ ss through the interaction between the CTD of RBFOX2 and the zinc finger domain of U1C, thus providing a molecular mechanism for the function of this splicing regulator.

RBFOX2 localizes to splicing factor-rich nuclear speckles via the C-terminal domain. Having demonstrated that the RBFOX2 CTD interacts with U1C, we looked to elucidate which portions of the protein were required for regulating exon choice. We first examined the localization of RBFOX2 domains. Splicing factors predominantly reside within the nucleus. An RBFOX2-specific antibody confirmed that endogenous RBFOX2 localized predominantly in the nuclear speckles as a punctate structure (Fig. 8, Endo Fox2). Within the nucleus, nuclear speckles function as storage compartments that supply splicing factors to active transcription sites when needed. Splicing factor SC35 also localized to the nuclear speckles. Superimposition of RBFOX2 and SC35 revealed that both proteins were intensely colocalized in the same region (Fig. 8, Endo Fox2).

To further characterize the RBFOX2 domain responsible for speckle localization, we expressed a full-length RBFOX2 as well as its individual NTD, RRM, or CTD fused with enhanced green fluorescent protein (EGFP) in HeLa cells and analyzed their localizations relative to SC35. Localization of the full-length RBFOX2 was similar to that of endogenous RBFOX2; it colocalized with SC35 in nuclear speckles (Fig. 8, Fox2-FL). A different localization pattern was observed for the NTD- and RRM-EGFP fusions. Both domains were diffusely localized throughout the nucleus without any apparent preference for accumulation on the speckles (Fig. 8, Fox2-NTD and Fox2-RRM). In addition, the RRM domain also localized to the cytoplasm. The CTD produced a speckle pattern within the nucleus that coincided with that of SC35 (Fig. 8, Fox2-CTD). Therefore, the CTD of RBFOX2 is responsible for targeting RBFOX2 to the nuclear speckle.

Functional RBFOX2 requires both the RRM and CTD. Having characterized its role in localization, we next sought to determine whether the CTD was required for regulating exon 16 splicing. The full-length RBFOX2 and its deletion mutant expression plasmids (Fig. 7A) were cotransfected in separate experiments with the exon 16 minigene into MELC and analyzed for exon 16 splicing patterns. The proteins were expressed at similar levels (Fig. 9A, anti-FLAG [α-FLAG]). Functionality of the protein was determined by the ability of the expressed proteins to change exon 16 splicing patterns.

Exon 16 inclusion from the vector served as a control. The expression of full-length RBFOX2 and RBFOX2 lacking the NTD domain (ΔNTD) increased exon 16 inclusion and resulted in ~68.1% and ~42.8% positive changes over that of the control vector, respectively (Fig. 9A). On the other hand, expression of RRM- or CTD-deleted RBFOX2 proteins (ΔRRM and ΔCTD) drastically reduced exon 16 inclusion and led to ~25.9% and ~22.9% negative changes, respectively, compared with that of the control vector alone. When the CTD was expressed, it exerted a strong negative effect, with an ~26.1% change in exon 16 inclusion (Fig. 9A). The bar graph reflects the percentages of exon 16 change relative to the control vector (Fig. 9B).

These results suggest that the NTD has a positive effect on RBFOX2 activity in exon 16 choice, albeit a smaller one. However, both the RRM and CTD are required for the proper regulation of exon 16 choice. Binding of RBFOX2 to the UGCAUG motifs downstream of the target exon may help recruitment of U1 snRNP to the weak 5′ ss through its interaction with U1C. The physiological importance of RBFOX2 and U1C interaction is evidenced by the dominant negative effects of ΔCTD or CTD overexpression on exon 16 splicing.

To obtain more direct evidence that the RBFOX2-CTD interaction is sufficient for exon 16 splicing enhancement, we analyzed its function in a bacteriophage MS2 coat protein recruitment system (10). In this system, the RBFOX2-binding sites of exon 16 minigene were replaced with three copies of the binding site for the MS2 coat protein (Fig. 10A), and the full-length RBFOX2 and its deletion domains were fused with MS2 protein. The effects of the full-length RBFOX2 and its deletion mutants were then analyzed in transfected cells. Minigene PTB that had neither an

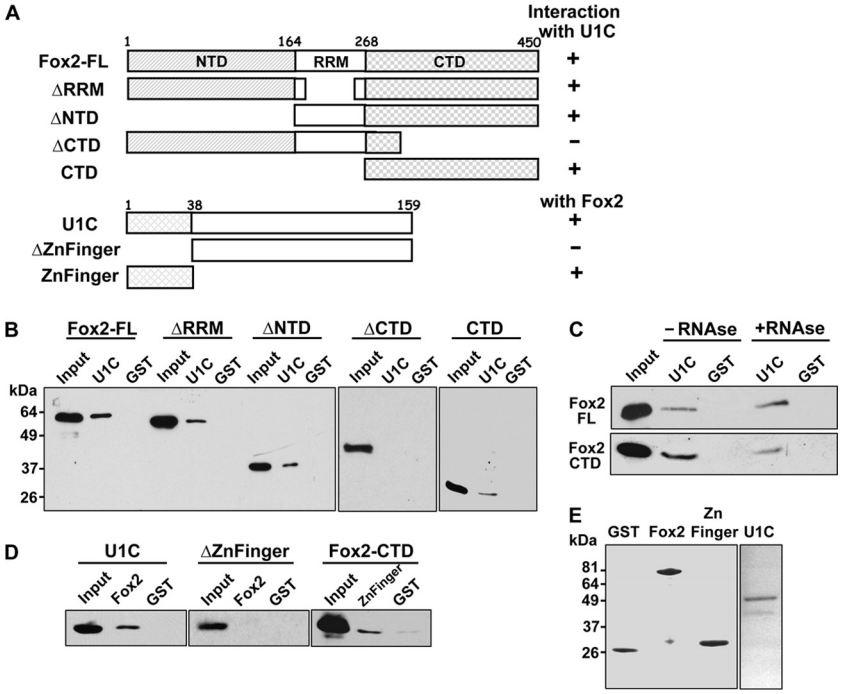

FIG 7 Interaction of RBFOX2 and U1C involves the CTD of RBFOX2 and the zinc finger domain of U1C. (A) Schematic of RBFOX2, U1C, and their deletion derivatives used for GST pulldown assays. Amino acid numbers for RBFOX2 and U1C are indicated. The names of the plasmids that encode each construct are given to the left of each diagram. (B) RBFOX2 containing the CTD or CTD by itself is sufficient for its interaction with U1C. RBFOX2 and its domain deletion variants expressed as FLAG fusion proteins were purified from transfected HEK293 cells and assayed for interaction with U1C expressed as a GST fusion in GST pulldown assays. (C) The interaction between RBFOX2 and U1C is RNA independent. Western blot analysis of GST pulldown assays in the absence (-) or presence (+) of RNase. Input, FLAG fusions purified from HEK293 cells. (D) The zinc finger region of U1C interacts with RBFOX2. U1C and U1C-ΔZnFinger expressed as FLAG fusions were analyzed for their interactions with Fox2-GST. As the small molecular mass of U1C-ZnFinger when expressed as a FLAG fusion made it difficult to detect it by Western analysis, it was expressed as a GST fusion (ZnFinger) and analyzed for its interaction with Fox2-CTD/FLAG. (E) Coomassie blue staining of purified GST, Fox2/GST, ZnFinger/GST, and U1C/GST proteins used in the experiment and separated on an SDS-polyacrylamide gel.

RBFOX2- nor MS2-binding site was cotransfected with Fox2-MS2 fusions and served as a control.

The construct Ex16-MS2 had the RBFOX2-binding sites replaced by tandem MS2 sites (Fig. 10A), and when transfected alone into HeLa cells gave low basal levels (~22%) of exon 16 inclusion (Fig. 10A). Cotransfection of Fox2-FL-MS2 produced high levels (~77%) of exon 16 inclusion. The three deletion constructs (ΔRRM, ΔNTD, and CTD) in which the CTD was preserved had activity levels nearly equivalent to that of the Fox2-FL-MS2 and with 71.3%, 68.5%, and 72.3% inclusion, respectively (Fig. 10A). In contrast, ΔCTD-MS2 fusions exerted nearly no effect on Ex16-MS2 splicing with ~27% of exon 16 inclusion (Fig. 10A). The expression of Fox2-FL-MS2 or its domain deletion MS2 fusions did not affect the splicing pattern of the PNB minigene (Fig. 10B), which lacked the binding sites for either RBFOX2 or MS2 coat protein. These results support our model that RBFOX2-CTD is sufficient to activate the 5′ ss.

Together, these data suggest a novel mechanism for exon 16 5′ ss activation, in which the binding of RBFOX2 to the downstream intronic splicing enhancer UGCAUG stabilizes the pre-mRNA–U1 snRNP complex through interactions with U1C (Fig. 11).

DISCUSSION

The present study implicates a novel splicing mechanism for RBFOX2, which exerts its effect through downstream intronic splicing enhancers to modulate protein 4.1R exon 16 expression. When bound to downstream UGCAUG elements, RBFOX2 stimulates exon 16 inclusion by facilitating recognition of the weak 5′ ss by U1 snRNP through its direct interaction with U1C. Thus, we suggest that RBFOX2 regulation takes place in the earliest steps of spliceosome assembly, which commit pre-mRNAs to the splicing pathway.

UGCAUG has long been known to activate splicing when present downstream of the target exon; however, no direct mechanisms have been characterized. Our studies showed that the contribution of RBFOX2 becomes negligible when UGCAUG is associated with a strong 5′ ss or when base-pairing complementarity between exon 16 5′ ss and U1 snRNA is improved. The correlation between the positive effect of RBFOX2 and the presence of a weak 5′ ss suggests that RBFOX2 either directly or indirectly targets protein components involved in the strengthening or stabilization of the weak 5′ ss. Even though splicing regulation occurs at every step throughout the assembly pathway, many factors enhance splicing in the presence of a weak 5′ ss by recruiting U1 snRNP to the 5′ ss. Binding of RBM25 with Bcl-X exonic element, CGGGCA, stabilizes the pre-mRNA–U1 snRNP through interactions with hLuc7A and activates the Bcl-x_s 5′ ss (50). SR proteins direct 5′ ss selection by regulation of the U1 snRNP assembly onto the pre-mRNA (48). RBFOX2 exerts no enhancing effect once U1 is bound to a strong 5′ ss. In agreement with the idea that regulation often occurs at the early step of spliceosome assembly, RBFOX2 recruits U1 snRNP to the weak exon 16 5′ ss.

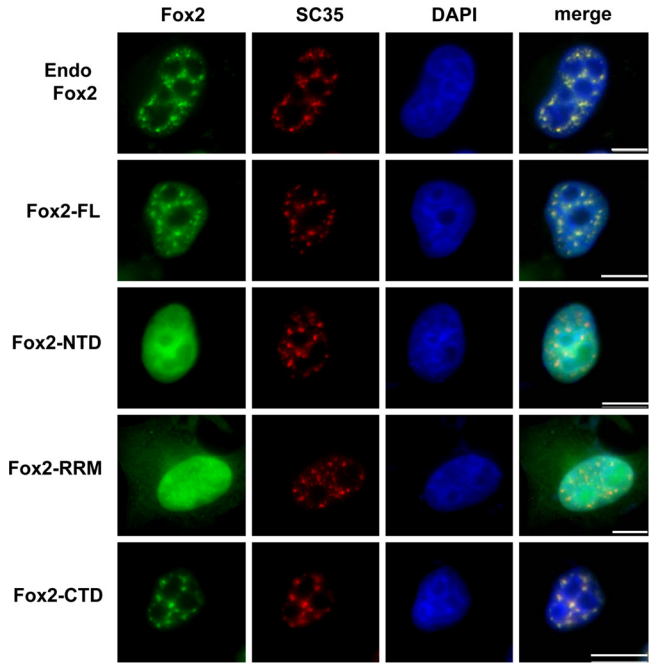

FIG 8 The CTD is critical for RBFOX2 localization to nuclear speckles. For endogenous RBFOX2 localization, HeLa cells were processed for immunofluorescence analysis with antibodies directed against RBFOX2 or SC35 and revealed with fluorescein isothiocyanate- or Alexa-conjugated secondary antibody, respectively. To identify the domain for nuclear speckle localization, RBFOX2 full length (FL), NTD, RRM, or CTD fused with EGFP were transfected into HeLa cells. The expressed EGFP fusion proteins were analyzed for localization relative to splicing factor SC35. Cells were fixed and stained with anti-SC35 antibody and DAPI. Bar, 10 μm.

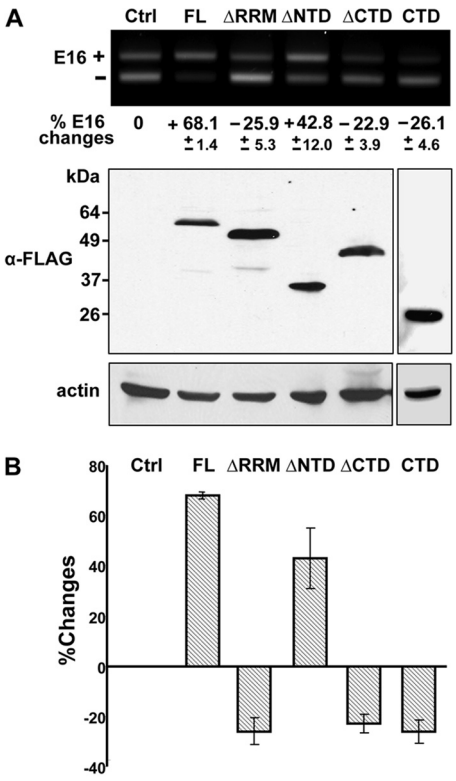

FIG 9 Both the RRM and CTD of RBFOX2 are required for exon 16 inclusion. (A) Inclusion of exon 16 in MELC is repressed by RBFOX2 deletion mutants lacking the RRM or CTD. (Upper panel) RT-PCR analyses of exon 16 expression from MELC transfected with the exon 16 minigene with control vector alone, full-length RBFOX2, or its deletion mutants. Products and percentages of exon 16 change are indicated below each lane. (Middle panel) Western blot analysis with an anti-FLAG antibody indicates the levels of exogenously expressed full-length RBFOX2 and its deletion derivatives following transfection. β-Actin served as a loading control. (B) The bar graph presents the percentages of exon 16 change relative to the control vector from the three experiments performed (means ± standard deviations).

The identification of the association between RBFOX2 and U1C provides insight into the mechanisms of RBFOX2 splicing activation. Binding of RBFOX2 to an intronic sequence (UGC AUG) could activate a weak 5′ ss through its interaction with U1C, which directly binds to the U1 snRNP necessary for 5′ ss recognition. Several other proteins have been shown to interact with U1C and have been implicated in splicing regulation (13, 35, 36). Thus, RBFOX2 joins a growing number of proteins that have been characterized as U1C-dependent splicing modulators.

U1C does not directly bind to the U1 snRNA; in fact, the binding of U1C to the U1 snRNP core domain is mediated by U1 70K. There is evidence that U1C is required for stable interaction between U1 snRNP and the pre-mRNA 5′ ss (17). U1C carries a cystidine/histidine zinc finger-like motif at its N terminus, which is necessary and sufficient for its binding to the U1 snRNP (32) as well as for homodimerization (15). The zinc finger-like motif containing region is required for U1C interaction with RBFOX2. This activity is reminiscent of TIA-1, which regulates splicing by binding to the N-terminal region of U1C (13). Whether the zinc finger-like motif is critical for RBFOX2 binding remains to be determined.

RBFOX2 contains an RNA-binding domain conserved among the different Fox family members and present in nearly all splice variants (1). In contrast, the flanking N- and C-terminal domains are not as highly conserved and do not show significant similarity to any other protein motifs in current databases. Both the NTD and RRM localize to the nucleus, while the CTD is responsible for nuclear speckle localization. A nuclear localization signal was identified at the NTD (KRPR at aa 46 to 49) by using an NLS program (http://www.predictprotein.org/); however, no other known NLS was found in the RRM and CTD. How these domains enter the nucleus remains to be determined. It has been shown that the arginine/serine-rich domain (RS) of SR proteins (6) and arginine/asparate-rich (RD) and arginine/glutamate-rich (RE) domains of RBM25 (50) mediate proper speckle localization. A novel sequence within the RBFOX2 CTD may thus serve as a targeting signal to nuclear speckles.

Both the RRM and CTD are critical for functional RBFOX2 in exon 16 splicing. Our results suggest that the interaction of U1C with the CTD region of RBFOX2 is critical for the recruitment of U1 snRNP to the weak 5′ ss. Interestingly, the CTD of RBFOX2 has also been suggested to be important for fibroblast growth factor receptor 2 exon IIIb activation and exon IIIc repression (3). The binding partners for the CTD domain and the molecular mechanisms involved in the repression and activation of these exons have not yet been characterized. It is conceivable that the RBFOX2 CTD could also interact with factors other than U1C.

Similar to protein 4.1R exon 16, exon inclusion in fibronectin EIIIB (25), the c-src N1 exon (31, 45), CaV1.2 L-type calcium channel exon 33 (43), PTBP1 exon 9a (47), and human ENAH

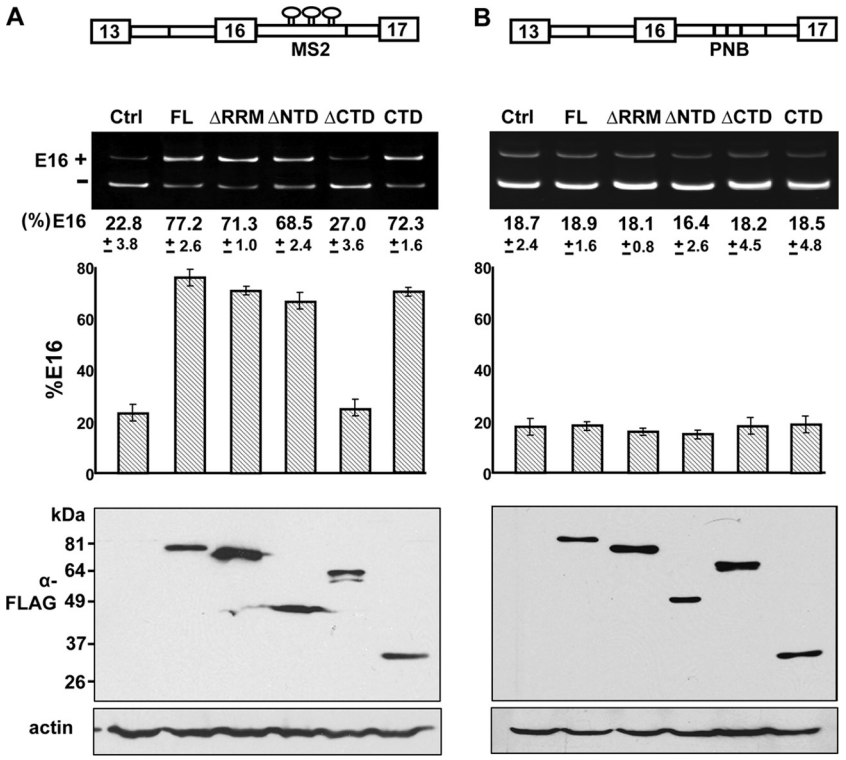

FIG 10 RBFOX2 CTD is sufficient to activate exon 16 (Ex16) splicing in an MS2 coat protein recruitment system. (A) Fox2-MS2 and its deletion derivatives that preserved the CTD exerted a positive effect on exon 16 splicing. (Upper panel) Schematic of Ex16-MS2 reporter with MS2-binding sites in place of RBFOX2-binding sites. (RT-PCR panel) The Ex16-MS2 reporter was cotransfected with Fox2-MS2 or its deletion derivatives into HeLa cells. RNAs were isolated and analyzed for exon 16 expression. Mean values ± standard deviations (SD) of three independent experiments are shown. (Bar graph) Percentages of exon 16 inclusion from the three experiments performed (means ± SD). (%) E16 is the percentage of spliced products that include exon 16. (Western blot panel) Anti-FLAG detected the expression of exogenous RBFOX2 and the indicated deletion proteins. β-Actin served as the loading control. (B) Fox2-MS2 or its deletion derivatives exerted no effect on exon 16 splicing in the PNB reporter. Similar analyses as performed for panel A were performed on Ex16-PNB minigene cotransfected with the same Fox2-MS2 and its deletion derivatives into HeLa cells.

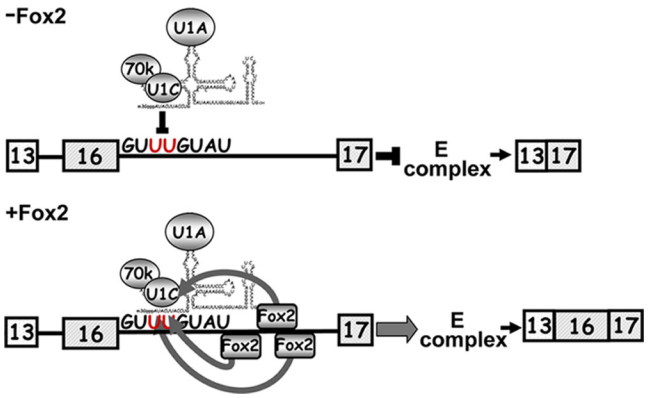

FIG 11 A mechanism for RBFOX2-mediated recruitment of U1 snRNP to weak 5′ ss followed by UGCAUG sequences. In the absence of RBFOX2, the weak 5′ ss is poorly recognized by U1 snRNP. This prevents E complex formation and results in exon 16 exclusion. In the presence of RBFOX2, RBFOX2 binds to the UGCAUG enhancer elements downstream of the target exon through its RRM and interacts with the zinc finger domain of U1C through its CTD. These interactions help to recruit and stabilize U1 snRNP to the weak 5′ ss. This results in spliceosome commitment complex formation and exon inclusion.

exon 12 (47) are induced by RBFOX2 proteins via the UGCAUG enhancer elements in the downstream intron. Analysis of the strength of the 5′ and 3′ ss of these UGCAUG-dependent exons revealed no consistent trends. Thus, whether RBFOX2 exerts similar functional activity on the splicing of these exons is yet to be determined.

An alternatively spliced exon is generally under the control of multiple splicing regulators, and it is likely that these exons are affected by various splicing factors in addition to RBFOX2. RBFOX2-binding sites are located in a downstream intronic region, which could possibly include binding sites for other proteins. Indeed, we found that PTB-binding sites situated between the 5′ ss and RBFOX2-binding sites also affected exon 16 splicing (data not shown). In a particular cellular context, regulation of alternative exon splicing will likely be dictated by the coordinated contribution of both *cis*- and *trans*-acting factors.

Our current working model for protein 4.1R exon 16 splicing (Fig. 11) is that binding of RBFOX2 to the downstream intronic binding sites stabilizes or increases U1 snRNP recruitment to the weak 5′ ss through a direct interaction between its CTD and the zinc finger domain of U1C. RBFOX2 thus participates in the earliest steps of splicesome assembly, committing pre-mRNAs to the splicing pathway. RBFOX2 expression has been found to be regulated during erythroid differentiation (46). Changes in the expression of RBFOX2 may influence efficiency in the utilization of a

weak 5′ ss and provide an orderly pathway to modulate splicing patterns. Furthermore, RBFOX2 target exons are widespread among erythroid genes (5), and the elucidation of 4.1R exon 16 regulation is critical for a better understanding of the regulated expression of other key erythroid genes.

ACKNOWLEDGMENTS

We thank D. L. Black (University of California, Los Angeles, CA) for the DUP4-1 minigene and R. Breathnach (Université de Nantes, Nantes, France) for the MS2 coat protein plasmid pCIMS2-NLS-FLAG. We thank W. Y. Tarn (Institute of Biomedical Sciences, Academia Sinica, Taipei, Taiwan) and Jane Wu (Northwestern University, Feinberg School of Medicine, Chicago, IL) for valuable suggestions.

This work was supported by NIH grant HL24385 (to E.J.B.) and the Claudia Barr Award (to S.C.H.).

REFERENCES

1. **Auweter SD, et al.** 2006. Molecular basis of RNA recognition by the human alternative splicing factor Fox-1. EMBO J. **25**:163–173.
2. **Baklouti F, Jr., et al.** 1996. Asynchronous regulation of splicing events within protein 4.1 pre-mRNA during erythroid differentiation. Blood **87**: 3934–3941.
3. **Baraniak AP, Chen JR, Garcia-Blanco MA.** 2006. Fox-2 mediates epithelial cell-specific fibroblast growth factor receptor 2 exon choice. Mol. Cell. Biol. **26**:1209–1222.
4. **Black DL.** 2003. Mechanisms of alternative pre-messenger RNA splicing. Annu. Rev. Biochem. **72**:291–336.
5. **Brudno M, et al.** 2001. Computational analysis of candidate intron regulatory elements for tissue-specific alternative pre-mRNA splicing. Nucleic Acids Res. **29**:2338–2348.
6. **Cazalla D, et al.** 2002. Nuclear export and retention signals in the RS domain of SR proteins. Mol. Cell. Biol. **22**:6871–6882.
7. **Chasis JA, et al.** 1993. Differentiation-associated switches in protein 4.1 expression. Synthesis of multiple structural isoforms during normal human erythropoiesis. J. Clin. Invest. **91**:329–338.
8. **Das R, Reed R.** 1999. Resolution of the mammalian E complex and the ATP-dependent spliceosomal complexes on native agarose mini-gels. RNA **5**:1504–1508.
9. **Deguillien M, et al.** 2001. Multiple cis elements regulate an alternative splicing event at 4.1R pre-mRNA during erythroid differentiation. Blood **98**:3809–3816.
10. **Del Gatto-Konczak F, Olive M, Gesnel MC, Breathnach R.** 1999. hnRNP A1 recruited to an exon in vivo can function as an exon splicing silencer. Mol. Cell. Biol. **19**:251–260.
11. **Dignam JD, Lebovitz RM, Roeder RG.** 1983. Accurate transcription initiation by RNA polymerase II in a soluble extract from isolated mammalian nuclei. Nucleic Acids Res. **11**:1475–1489.
12. **Discher D, Parra M, Conboy JG, Mohandas N.** 1993. Mechanochemistry of the alternatively spliced spectrin-actin binding domain in membrane skeletal protein 4.1. J. Biol. Chem. **268**:7186–7195.
13. **Forch P, Puig O, Martinez C, Seraphin B, Valcarcel J.** 2002. The splicing regulator TIA-1 interacts with U1-C to promote U1 snRNP recruitment to 5′ splice sites. EMBO J. **21**:6882–6892.
14. **Fukumura K, et al.** 2007. Tissue-specific splicing regulator Fox-1 induces exon skipping by interfering E complex formation on the downstream intron of human F1γ gene. Nucleic Acids Res. **35**:5303–5311.
15. **Gunnewiek JM, et al.** 1995. Homodimerization of the human U1 snRNP-specific protein C. Nucleic Acids Res. **23**:4864–4871.
16. **Hedjran F, Yeakley JM, Huh GS, Hynes RO, Rosenfeld MG.** 1997. Control of alternative pre-mRNA splicing by distributed pentameric repeats. Proc. Natl. Acad. Sci. U. S. A. **94**:12343–12347.
17. **Heinrichs V, Bach M, Winkelmann G, Luhrmann R.** 1990. U1-specific protein C needed for efficient complex formation of U1 snRNP with a 5′ splice site. Science **247**:69–72.
18. **Horne WC, Huang SC, Becker PS, Tang TK, Benz EJ, Jr.** 1993. Tissue-specific alternative splicing of protein 4.1 inserts an exon necessary for formation of the ternary complex with erythrocyte spectrin and F-actin. Blood **82**:2558–2563.
19. **Horowitz DS, Krainer AR.** 1994. Mechanisms for selecting 5′ splice sites in mammalian pre-mRNA splicing. Trends Genet. **10**:100–106.
20. **Huh GS, Hynes RO.** 1994. Regulation of alternative pre-mRNA splicing by a novel repeated hexanucleotide element. Genes Dev. **8**:1561–1574.
21. **Izquierdo JM, et al.** 2005. Regulation of Fas alternative splicing by antagonistic effects of TIA-1 and PTB on exon definition. Mol. Cell **19**:475–484.
22. **Jin Y, et al.** 2003. A vertebrate RNA-binding protein Fox-1 regulates tissue-specific splicing via the pentanucleotide GCAUG. EMBO J. **22**: 905–912.
23. **Jurica MS, Moore MJ.** 2003. Pre-mRNA splicing: awash in a sea of proteins. Mol. Cell **12**:5–14.
24. **Kawamoto S.** 1996. Neuron-specific alternative splicing of nonmuscle myosin II heavy chain-B pre-mRNA requires a cis-acting intron sequence. J. Biol. Chem. **271**:17613–17616.
25. **Lim LP, Sharp PA.** 1998. Alternative splicing of the fibronectin EIIIB exon depends on specific TGCATG repeats. Mol. Cell. Biol. **18**: 3900–3906.
26. **Maniatis T, Tasic B.** 2002. Alternative pre-mRNA splicing and proteome expansion in metazoans. Nature **418**:236–243.
27. **Mauger DM, Lin C, Garcia-Blanco MA.** 2008. hnRNP H and hnRNP F complex with Fox2 to silence fibroblast growth factor receptor 2 exon IIIc. Mol. Cell. Biol. **28**:5403–5419.
28. **Merendino L, Guth S, Bilbao D, Martinez C, Valcarcel J.** 1999. Inhibition of msl-2 splicing by sex-lethal reveals interaction between U2AF35 and the 3′ splice site AG. Nature **402**:838–841.
29. **Michaud S, Reed R.** 1993. A functional association between the 5′ and 3′ splice site is established in the earliest prespliceosome complex (E) in mammals. Genes Dev. **7**:1008–1020.
30. **Minovitsky S, Gee SL, Schokrpur S, Dubchak I, Conboy JG.** 2005. The splicing regulatory element, UGCAUG, is phylogenetically and spatially conserved in introns that flank tissue-specific alternative exons. Nucleic Acids Res. **33**:714–724.
31. **Modafferi EF, Black DL.** 1997. A complex intronic splicing enhancer from the c-src pre-mRNA activates inclusion of a heterologous exon. Mol. Cell. Biol. **17**:6537–6545.
32. **Nelissen RL, et al.** 1991. Zinc finger-like structure in U1-specific protein C is essential for specific binding to U1 snRNP. Nucleic Acids Res. **19**:449–454.
33. **Nilsen TW.** 2002. The spliceosome: no assembly required? Mol. Cell **9**:8–9.
34. **Norton PA.** 1994. Alternative pre-mRNA splicing: factors involved in splice site selection. J. Cell Sci. **107**:1–7.
35. **Ohkura N, Takahashi M, Yaguchi H, Nagamura Y, Tsukada T.** 2005. Coactivator-associated arginine methyltransferase 1, CARM1, affects pre-mRNA splicing in an isoform-specific manner. J. Biol. Chem. **280**: 28927–28935.
36. **Ohkura N, Yaguchi H, Tsukada T, Yamaguchi K.** 2002. The EWS/NOR1 fusion gene product gains a novel activity affecting pre-mRNA splicing. J. Biol. Chem. **277**:535–543.
37. **Ponthier JL, et al.** 2006. Fox-2 splicing factor binds to a conserved intron motif to promote inclusion of protein 4.1R alternative exon 16. J. Biol. Chem. **281**:12468–12474.
38. **Rinke J, Appel B, Blocker H, Frank R, Luhrmann R.** 1984. The 5′-terminal sequence of U1 RNA complementary to the consensus 5′ splice site of hnRNA is single-stranded in intact U1 snRNP particles. Nucleic Acids Res. **12**:4111–4126.
39. **Sergeant KA, et al.** 2007. Alternative RNA splicing complexes containing the scaffold attachment factor SAFB2. J. Cell Sci. **120**:309–319.
40. **Shapiro MB, Senapathy P.** 1986. Automated preparation of DNA sequences for publication. Nucleic Acids Res. **14**:65–73.
41. **Stetefeld J, Ruegg MA.** 2005. Structural and functional diversity generated by alternative mRNA splicing. Trends Biochem. Sci. **30**:515–521.
42. **Takakuwa Y, Tchernia G, Rossi M, Benabadji M, Mohandas N.** 1986. Restoration of normal membrane stability to unstable protein 4.1-deficient erythrocyte membranes by incorporation of purified protein 4.1. J. Clin. Invest. **78**:80–85.
43. **Tang ZZ, Zheng S, Nikolic J, Black DL.** 2009. Developmental control of CaV1.2 L-type calcium channel splicing by Fox proteins. Mol. Cell Biol. **29**:4757–4765.
44. **Tchernia G, Mohandas N, Shohet SB.** 1981. Deficiency of skeletal membrane protein band 4.1 in homozygous hereditary elliptocytosis. Implications for erythrocyte membrane stability. J. Clin. Invest. **68**:454–460.
45. **Underwood JG, Boutz PL, Dougherty JD, Stoilov P, Black DL.** 2005. Homologues of the Caenorhabditis elegans Fox-1 protein are neuronal splicing regulators in mammals. Mol. Cell. Biol. **25**:10005–10016.
46. **Yang G, Huang SC, Wu JY, Benz EJ, Jr.** 2008. Regulated Fox-2 isoform

expression mediates protein 4.1R splicing during erythroid differentiation. Blood **111**:392–401.
47. **Yeo GW, et al.** 2009. An RNA code for the FOX2 splicing regulator revealed by mapping RNA-protein interactions in stem cells. Nat. Struct. Mol. Biol. **16**:130–137.
48. **Zahler AM, Roth MB.** 1995. Distinct functions of SR proteins in recruitment of U1 small nuclear ribonucleoprotein to alternative 5′ splice sites. Proc. Natl. Acad. Sci. U. S. A. **92**:2642–2646.
49. **Zhang C, et al.** 2008. Defining the regulatory network of the tissue-specific splicing factors Fox-1 and Fox-2. Genes Dev. **22**:2550–2563.
50. **Zhou A, Ou AC, Cho A, Benz EJ, Jr., Huang SC.** 2008. Novel splicing factor RBM25 modulates Bcl-x pre-mRNA 5′ splice site selection. Mol. Cell. Biol. **28**:5924–5936.
51. **Zhou HL, Baraniak AP, Lou H.** 2007. Role for Fox-1/Fox-2 in mediating the neuronal pathway of calcitonin/calcitonin gene-related peptide alternative RNA processing. Mol. Cell. Biol. **27**:830–841.
52. **Zhu H, Hasman RA, Young KM, Kedersha NL, Lou H.** 2003. U1 snRNP-dependent function of TIAR in the regulation of alternative RNA processing of the human calcitonin/CGRP pre-mRNA. Mol. Cell. Biol. **23**:5959–5971.